

plexes. The frequencies of the ν_1 , ν_4 , and ν_6 absorptions might well be used to assign the oxidation state of a complexed lanthanide or actinide in the unlikely event of its being in doubt. The infrared spectrum of $\text{CsPa}(\text{NO}_3)_6$ ²⁶ supports this possibility. In this context, the uranyl ion behaves both in some chemical properties and as regards the infrared spectra of its nitrate complexes²⁷ as if it were $^-\text{O}-\text{U}^{4+}-\text{O}^-$.

The effect of coordination on the P–O frequency of phosphine oxides has been discussed previously.²⁸ The shift to low frequency is here much greater than observed^{3,23} for lanthanide(III) complexes and similar to that observed² for U(IV), and we attribute the additional shift to delocalization of the P–O π -electron density into the metal 5d (Ce) or 6d (Th) orbitals.

(26) D. Brown and P. I. Jones, *J. Chem. Soc. A*, 733 (1966).

(27) F. A. Hart and J. E. Newberry, *J. Inorg. Nucl. Chem.*, **28**, 1334 (1966).

(28) F. A. Cotton, R. D. Barnes, and E. Bannister, *J. Chem. Soc.*, 2199 (1960).

However, the mean P–O distance of 1.53 Å indicates that this link still possesses considerable double-bond character. It is relevant that the lanthanide contraction increases the P–O frequency along the series La(III)–Lu(III),²³ suggesting that metal–oxygen π bonding is here unimportant, compared with coupling with the metal–oxygen bond and the inductive effect on the P–O σ bond. Indeed, the generally accepted view that there is little covalent character in lanthanide compounds but moderate covalent character in actinide compounds probably reflects not so much the difference in principal quantum number as the difference in commonly occurring oxidation states.

Acknowledgments.—We wish to thank the National Institutes of Health for Grant GM-08395-09 and NSF for Grant GP-8301. We also wish to thank Montana State University for grants which have made possible the computing required for this study.

CONTRIBUTION FROM THE DEPARTMENT OF CHEMISTRY AND CHEMICAL ENGINEERING AND MATERIALS RESEARCH LABORATORY, UNIVERSITY OF ILLINOIS, URBANA, ILLINOIS 61801

A Structural Study of Two Products of the Reaction of Phosphorus Pentachloride with Titanium Tetrachloride. The Crystal and Molecular Structures of Bis(tetrachlorophosphonium) Di- μ -chloro-octachlorodititanate(IV), $[\text{PCl}_4]_2[\text{Ti}_2\text{Cl}_{10}]$, and Tetrachlorophosphonium Tri- μ -chloro-hexachlorodititanate(IV), $[\text{PCl}_4][\text{Ti}_2\text{Cl}_9]$ ^{1a}

By T. J. KISTENMACHER^{1b} AND G. D. STUCKY*

Received October 31, 1969

Reaction of PCl_5 with TiCl_4 in POCl_3 has led to a crystalline product of empirical formula PTiCl_9 . The crystal system is triclinic, space group $C_1^1-P\bar{1}$. The cell constants for the reduced cell are $a = 8.919$ (1) Å, $b = 9.474$ (1) Å, $c = 6.913$ (1) Å, $\alpha = 95.90$ (1)°, $\beta = 95.90$ (1)°, and $\gamma = 100.98$ (1)°. The calculated density of 2.34 g/cm³ for 2 PTiCl_9 formula units per cell is to be compared to the observed density of 2.32 ± 0.02 g/cm³. Of 3387 independent reflections collected by counter methods, 2571 were considered to be observed and were used to refine the structure by full-matrix least squares to a conventional R factor of 6.9%. The structure consists of PCl_4^+ and edge-bridged bioctahedral $\text{Ti}_2\text{Cl}_{10}^{2-}$ ions, the latter located on crystallographic centers of inversion. Reaction of a solution of PCl_5 in SOCl_2 with TiCl_4 in SOCl_2 led to a crystalline product of empirical formula $\text{PTi}_2\text{Cl}_{13}$. The crystal system is orthorhombic with possible space groups $D_{2h}^{16}-Pnma$ or $C_{2v}^9-Pn2_1a$. The cell constants are $a = 29.126$ (12) Å, $b = 10.521$ (2) Å, and $c = 11.514$ (3) Å. The calculated density for eight $\text{PTi}_2\text{Cl}_{13}$ formula units per cell is 2.22 g/cm³ and the observed density is 2.28 ± 0.04 g/cm³. A total of 1950 counter-collected observed and unobserved reflections were used to refine the structure by full-matrix least squares to a conventional R factor of 7.6%, assuming space group $Pnma$. Some indication of disorder or lower space group symmetry was found. The structure consists of PCl_4^+ and Ti_2Cl_9^- ions. The anions are an unusual example of face-shared bioctahedra containing first-row transition metal ions in the formal oxidation state +4.

Introduction

Adducts of the type $(\text{PCl}_5)_n \cdot m\text{TiCl}_4$, where n and m are integers, were first reported by Weber.² Treatment of a PCl_5 - TiCl_4 solution with Cl_2 gas led to the complex $\text{PCl}_5 \cdot \text{TiCl}_4$. In a series of experiments^{3–5} Groene-

veld studied the reaction of PCl_5 and TiCl_4 in POCl_3 and SOCl_2 . Addition of PCl_5 to a solution of TiCl_4 in POCl_3 produced the complex $\text{PCl}_5 \cdot \text{TiCl}_4$. Addition of PCl_5 to a solution of TiCl_4 in SOCl_2 was also reported to give the 1:1 adduct. Conductometric titration of a solution of TiCl_4 in POCl_3 with PCl_5 in POCl_3 indicated complexes of stoichiometry $\text{PCl}_5 \cdot \text{TiCl}_4$ and $2\text{PCl}_5 \cdot \text{TiCl}_4$. Only the 1:1 adduct was reported to be isolable. Payne⁶ found that the conductometric titration of TiCl_4 in CH_3CN with PCl_5 in CH_3CN

* To whom correspondence should be addressed.

(1) (a) This work was supported in part by the Advanced Research Projects Agency under Contract SD-131. (b) Union Carbide Corp. predoctoral fellow.

(2) R. Weber, *Pogg. Ann.*, **132**, 452 (1867).

(3) W. L. Groeneveld, *Recl. Trav. Chim. Pays-Bas*, **71**, 1152 (1952).

(4) W. L. Groeneveld and A. P. Zuur, *ibid.*, **72**, 617 (1953).

(5) W. L. Groeneveld, *ibid.*, **75**, 594 (1956).

(6) D. S. Payne, *ibid.*, **75**, 620 (1956).

showed a considerable increase in conductance at 1:1 and 2:1 ratios of PCl_5 to TiCl_4 . Neither complex was isolated.

We have reinvestigated the products formed by the reaction of PCl_5 and TiCl_4 in POCl_3 and SOCl_2 . The solid product formed in POCl_3 solution has been shown by X-ray structural analysis to be the 1:1 adduct. The structure consists of PCl_4^+ and edge-bridged bioctahedral $\text{Ti}_2\text{Cl}_{10}^{2-}$ ions. The solid reaction product formed from the reaction of a PCl_5 - SOCl_2 solution with a TiCl_4 - SOCl_2 solution, however, has the stoichiometry of $\text{PCl}_5 \cdot 2\text{TiCl}_4$. This structure consists of PCl_4^+ and the unusual face-shared bioctahedral Ti_2Cl_9^- ion. To the best of our knowledge this is the first X-ray structural study of a first-row transition metal ion with a formal charge of +4 existing in this configuration.

Experimental Section

All starting materials were reagent grade and used without further purification.

Addition of a solution of 2 g (20 mmol) of PCl_5 in 25 ml of POCl_3 (80°) to a solution of 2 ml (18 mmol) of TiCl_4 in 10 ml of POCl_3 (80°) initially produced a yellow-orange precipitate. The mixture was then brought to approximately 100° , and the mother liquor was decanted and allowed to cool. Yellow-orange plates of $[\text{PCl}_4]_2[\text{Ti}_2\text{Cl}_{10}]$ formed within a few hours. *Anal.* Calcd for PTiCl_9 : Ti, 12.0; Cl, 80.2. Found: Ti, 12.1; Cl, 78.7; Cl/Ti ratio, 8.8. Crystals for X-ray examination were mounted in thin-walled glass capillaries.

Addition of 4.8 ml (54 mmol) of PCl_5 to a solution of 2 ml (18 mmol) of TiCl_4 in 40 ml of SOCl_2 (1.3 ml of solvent is required for a 1:1 PCl_5 : TiCl_4 mole ratio⁷) produced bright yellow crystals of $[\text{PCl}_4][\text{Ti}_2\text{Cl}_9]$ in about 24 hr. *Anal.* Calcd for PTi_2Cl_9 : Ti, 16.3; Cl, 78.4. Found: Ti, 16.0; Cl, 74.9; Cl/Ti ratio, 6.4. The above results are an average of 16 different samples. Crystals for X-ray examination were mounted in thin-walled glass capillaries.

Both crystalline products were extremely water sensitive and all manipulations were carried out in a drybox under an argon atmosphere.

In a further experiment, it was found that addition of 2 g (20 mmol) of PCl_5 to 2 ml (18 mmol) of TiCl_4 in 25 ml of SOCl_2 at 70° yielded a yellow solution with a slight residue of PCl_5 remaining (PCl_5 itself has only limited solubility in SOCl_2). The mother liquor was decanted and allowed to cool. After about 24 hr, bright yellow crystals of $[\text{PCl}_4][\text{Ti}_2\text{Cl}_9]$ formed. *Anal.* Calcd for PTi_2Cl_9 : Ti, 16.3; Cl, 78.4. Found: Ti, 15.9; Cl, 75.6; Cl/Ti ratio, 6.4.

Collection and Reduction of the Intensity Data

Both sets of intensity data were collected on an automated Picker four-circle diffractometer equipped with a highly orientated graphite monochromator crystal. $\text{Mo K}\alpha$ radiation was used for intensity data collection. The θ - 2θ scan technique was used with a scan rate of $1^\circ/\text{min}$. Stationary-crystal, stationary-counter background counts of 10 sec were taken at the beginning and end of the scan. Lattice constants and standard deviations were obtained from a least-squares fit to the angular settings of 12 high-angle ($2\theta > 40^\circ$) reflections. Strips of copper foil were automatically inserted to attenuate the diffracted beam whenever the counting rate exceeded 10,000 cps. The

(7) The stoichiometry calculations were based on the reaction $3\text{PCl}_5 + \text{SOCl}_2 \rightarrow \text{PCl}_5 + \text{POCl}_3 + \text{PSCl}_3$ reported by P. H. Michaelis, *Jena. Z. Med. Naturwiss.*, **6**, 239 (1870).

raw intensities were corrected for background, Lorentz-polarization effects, and absorption.⁸ The polarization correction used for the monochromatic radiation was $(\cos^2 2\theta_m + \cos^2 2\theta)/(1 + \cos^2 2\theta_m)$ where θ_m is the Bragg angle of the monochromator crystal.

Unobserved reflections $[I_0 < 3[\sigma^2(I) + \sigma^2(\text{BKG})]^{1/2}]$, where I_0 is the background corrected peak count, $\sigma^2(I)$ the total integrated peak count in a scan time TC, and $\sigma^2(\text{BKG}) = (\text{TC}/\text{TB})^2(B_1 + B_2)$, with B_1 and B_2 the background counts in a time $\text{TB}/2$] were given a raw intensity of $[\sigma^2(I) + \sigma^2(\text{BKG})]^{1/2}$.

Preliminary optical and X-ray examination of the crystals of $[\text{PCl}_4]_2[\text{TiCl}_{10}]$ showed the crystal system to be triclinic. With the aid of the computer program TRACER,¹⁰ the reduced cell was determined and the reflections were indexed on the basis of this cell. The cell constants for the reduced cell are $a = 8.919 \pm 0.001 \text{ \AA}$, $b = 9.474 \pm 0.001 \text{ \AA}$, $c = 6.913 \pm 0.001 \text{ \AA}$, $\alpha = 95.90 \pm 0.01^\circ$, $\beta = 95.90 \pm 0.01^\circ$, $\gamma = 100.98 \pm 0.01^\circ$, and $V = 565.91 \text{ \AA}^3$ (28° , $\lambda(\text{Mo K}\alpha_1) 0.70926 \text{ \AA}$). The calculated density of 2.34 g/cm^3 for 2 PTiCl_9 formula units per cell agrees with the observed density of $2.32 \pm 0.02 \text{ g/cm}^3$ measured by flotation methods in a mixture of benzene and diiodomethane. The linear absorption coefficient for $\text{Mo K}\alpha$ radiation is 29.11 cm^{-1} .

The crystal mounted for intensity measurements was a parallelepiped with dimensions $0.13 \times 0.28 \times 0.38 \text{ mm}$ along b^* , c^* , and a^* , respectively. One form of data (hkl , $\bar{h}kl$, $hk\bar{l}$, $\bar{h}k\bar{l}$) was collected. The takeoff angle was set at 1.6° , where 75% of the maximum peak height as a function of takeoff angle was observed. A symmetrical scan range of 1.3° was taken about the position calculated for $\text{K}\alpha_1$. A full width at half-height measurement in an ω scan of a $\text{K}\alpha_1$ -resolved peak at 48° in 2θ was 0.12° indicating a satisfactorily low mosaic spread. Two standard reflections were collected following every 40 reflections. Both of their intensities had decreased by approximately 9% at the termination of the first form of data, and it was decided not to collect a second form. A correction curve was derived by averaging the drop in intensity of the two standards and fitting the resulting data points to a curve. The data in each interval of 40 reflections were scaled by the midpoint of the interval determined from this curve. A total of 3287 independent reflections were collected to 60° in 2θ . Of these, 2571 reflections were considered to be observed by the above criterion and were used in the structural refinement. The raw data were corrected for background, Lorentz-polarization effects, and absorption. The range of transmission factors was 0.63–0.74. Statistical tests¹¹ including both observed and

(8) D. J. Wehe, W. R. Busing, and H. A. Levy, "ORABS, a Fortran Program for Calculating Single-Crystal Absorption Corrections," USAEC Report ORNL-TM-229, Oak Ridge National Laboratory, Oak Ridge, Tenn., 1962.

(9) W. C. Hamilton, *Acta Crystallogr.*, **8**, 185 (1955).

(10) S. L. Lawton and R. A. Jacobson, "TRACER, a general Fortran Lattice Transformation-Cell Reduction Program," USAEC Report IS-1141, Ames Laboratory, Ames, Iowa, 1965.

(11) R. K. Dewar, A. L. Stone, and E. B. Fleischer, "Program FAME," private communication, 1966.

TABLE I
 POSITIONAL AND THERMAL PARAMETERS FOR $[\text{PCl}_4]_2[\text{Ti}_2\text{Cl}_{10}]$

Atom	<i>x</i>	<i>y</i>	<i>z</i>	B_{11}^a	B_{22}	B_{33}	B_{12}	B_{13}	B_{23}
Ti	0.3638 (2) ^b	0.3212 (1)	0.3856 (2)	0.0079 (2)	0.0053 (1)	0.0090 (3)	0.0010 (1)	0.0029 (2)	-0.0001 (1)
Cl(1)	0.5789 (2)	0.2210 (2)	0.3770 (3)	0.0099 (3)	0.0073 (2)	0.0133 (4)	0.0030 (2)	0.0036 (3)	0.0008 (2)
Cl(2)	0.1637 (2)	0.4380 (2)	0.4192 (3)	0.0086 (3)	0.0095 (2)	0.0174 (5)	0.0032 (2)	0.0031 (3)	0.0000 (3)
Cl(3)	0.2858 (3)	0.2459 (2)	0.0658 (3)	0.0119 (3)	0.0095 (2)	0.0100 (4)	0.0013 (2)	0.0012 (3)	-0.0010 (2)
Cl(4)	0.2401 (3)	0.1303 (2)	0.5202 (3)	0.0144 (3)	0.0072 (2)	0.0195 (5)	0.0001 (2)	0.0082 (3)	0.0030 (2)
Cl(5)	0.5157 (2)	0.5484 (2)	0.2894 (2)	0.0097 (2)	0.0057 (2)	0.0082 (3)	0.0011 (2)	0.0028 (2)	0.0013 (2)
P	0.1936 (2)	0.7774 (2)	0.0490 (3)	0.0089 (3)	0.0060 (2)	0.0104 (4)	0.0012 (2)	0.0033 (3)	0.0009 (2)
Cl(6)	0.2009 (3)	0.5846 (2)	-0.0620 (3)	0.0155 (4)	0.0058 (2)	0.0182 (5)	0.0020 (2)	0.0057 (3)	-0.0000 (2)
Cl(7)	0.0611 (3)	0.7666 (3)	0.2544 (3)	0.0125 (3)	0.0125 (3)	0.0144 (4)	0.0017 (2)	0.0073 (3)	0.0003 (3)
Cl(8)	0.1096 (3)	0.8781 (3)	-0.1527 (3)	0.0132 (3)	0.0103 (3)	0.0168 (5)	0.0038 (2)	0.0024 (3)	0.0042 (3)
Cl(9)	0.3969 (3)	0.8815 (2)	0.1561 (3)	0.0098 (3)	0.0108 (3)	0.0157 (4)	-0.0009 (2)	0.0011 (3)	0.0014 (3)

^a The form of the anisotropic ellipsoid is $\exp[-(B_{11}h^2 + B_{22}k^2 + B_{33}l^2 + 2B_{12}hk + 2B_{13}hl + 2B_{23}kl)]$. ^b Numbers in parentheses here and in succeeding tables are estimated standard deviations in the least significant digits.

unobserved data strongly indicated the centric triclinic space group $C_i^1-P\bar{1}$ as the correct space group. Weights $[1/\sigma^2(F_o)]$ were chosen from a Hughes scheme:¹²⁻¹⁴ $F_o \leq 4F_{\min}$, $\sigma(F_o) = 4F_{\min}/F_o$; $F_o > 4F_{\min}$, $\sigma(F_o) = F_o/4F_{\min}$, where F_{\min} was taken to be the magnitude of the minimum observed reflection.

Preliminary optical and X-ray examination of the crystals of $[\text{PCl}_4]_2[\text{Ti}_2\text{Cl}_{10}]$ showed that the crystal system was orthorhombic. The cell constants are $a = 29.126 \pm 0.012 \text{ \AA}$, $b = 10.521 \pm 0.002 \text{ \AA}$, $c = 11.514 \pm 0.003 \text{ \AA}$, and $V = 3528.29 \text{ \AA}^3$ (28° , $\lambda(\text{Mo K}\alpha) 0.71069 \text{ \AA}$). Systematic absences as determined by precession (Mo $K\alpha$) and Weissenberg (Cu $K\alpha$) photographs were $0kl$, $k + l \neq 2n$; $hk0$, $h \neq 2n$. These absences are consistent with the orthorhombic space groups D_{2h}^{16} - $Pnma$ (centric) or C_{2v}^9 - $Pn2_1a$ (acentric). The calculated density of 2.22 g/cm^3 for 8 $\text{PTi}_2\text{Cl}_{18}$ formula units per cell agrees fairly well with the observed density of $2.28 \pm 0.04 \text{ g/cm}^3$ measured by flotation methods in a mixture of iodomethane and diiodomethane. The linear absorption coefficient for Mo $K\alpha$ radiation is 30.32 cm^{-1} .

The crystal mounted for intensity measurements was a block with dimensions $0.11 \times 0.22 \times 0.37 \text{ mm}$ along a , c , and b , respectively. One form of data (hkl) was collected. The takeoff angle was set at 1.2° , where 70% of the maximum peak height as a function of takeoff angle was observed. A symmetrical scan of 1.4° was taken about the position calculated for $K\alpha$. A full width at half-height measurement in an ω scan of a $K\alpha$ peak at about 40° in 2θ was 0.20° and suggested a satisfactorily low mosaic spread. Two standard reflections were monitored after every 40 reflections. The intensities of both standards had decreased by approximately 25% at the termination of the hkl data set. During the course of data collection the crystal had to be realigned several times to correct for slippage. The crystals seem to be chemically unstable in the isolated environment of the capillary tube, and it was decided that this was as good a data set as could be obtained. A decomposition correction of the type described above was used to correct for the loss in intensity. The intensities of 3143 total

reflections were measured to 50° in 2θ . Elimination of reflections forbidden by symmetry and the unobserved data between 40 and 50° in 2θ left a data set of 1966 reflections of which 1163 were considered to be observed. The raw data were corrected for background, Lorentz-polarization, and absorption effects. The range of transmission factors was 0.54-0.72. Sixteen low-angle, high-intensity reflections which were extinction affected were eventually rejected from the data set. The results of statistical tests based on all reflections, observed and unobserved, were inconclusive but favored the centric space group $Pnma$. Weights $[1/\sigma^2(F_o)]$ were chosen from the Hughes¹²⁻¹⁴ scheme described above with F_{\min} taken as the magnitude of the minimum observed reflections of this data set.

In both structures the scattering factors for P^0 , Ti^0 , and Cl^0 were taken from the compilation of Hanson, Herman, Lea, and Skillman.¹⁵ Anomalous dispersion corrections ($\Delta f'$ and $\Delta f''$) were taken from Table 3.3.2c of the "International Tables for X-ray Crystallography," Vol. III, 1962, and applied to the calculated structure factors.

Solution and Refinement of the Structures¹⁶

(1) $[\text{PCl}_4]_2[\text{Ti}_2\text{Cl}_{10}]$.—There are two highly probable structural possibilities for the compound of empirical formula PTiCl_9 : (a) isolated PCl_4^+ and TiCl_5^- ions and (b) PCl_4^+ and $\text{Ti}_2\text{Cl}_{10}^{2-}$ ions. Possibility (b) is the most likely due to the known preference of Ti^{4+} for octahedral geometry. For two molecules of PTiCl_9 in the centric space group $P\bar{1}$ (a) would require one independent PCl_4^+ and one independent TiCl_5^- , while (b) would require one independent PCl_4^+ and a $\text{Ti}_2\text{Cl}_{10}^{2-}$ dimer located about one of the centers of inversion.

A Patterson solution was attempted, but a vector interpretation could not be made. The symbolic addi-

(15) H. P. Hanson, F. Herman, J. D. Lea, and S. Skillman, *ibid.*, **17**, 1040 (1964).

(16) Least-squares refinements, error analyses, and the thermal ellipsoid plots were calculated using local versions of the following programs: ORFLS, minimizing $\sum w(F_o - F_c)^2$, written by W. R. Busing, K. O. Martin, and H. A. Levy, 1962; ORFPE, written by W. R. Busing, K. O. Martin, and H. A. Levy, 1964; ORTEP, written by C. K. Johnson, Oak Ridge National Laboratory, Oak Ridge, Tenn., 1955. Patterson function, Fourier, and E map calculations were carried out with a Fourier Summation Program written by J. Gvildys, Argonne National Laboratory, Argonne, Ill., 1968.

(12) E. W. Hughes, *J. Amer. Chem. Soc.*, **63**, 1737 (1941).

(13) S. C. Abrahams and J. M. Reddy, *J. Chem. Phys.*, **43**, 2533 (1965).

(14) S. C. Abrahams, *Acta Crystallogr., Sect. A*, **25**, 165 (1969).

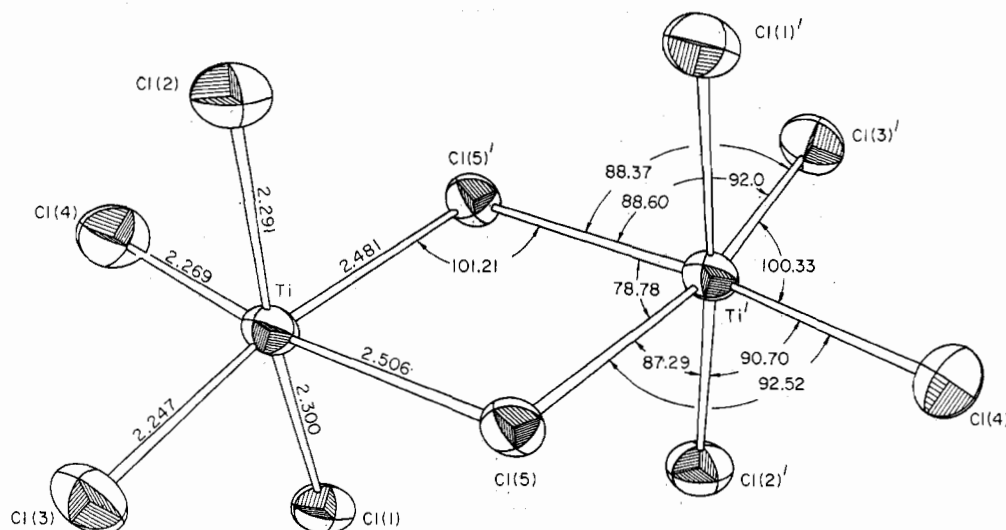


Figure 2.—A perspective view of the edge-bridged bioctahedral $\text{Ti}_2\text{Cl}_{10}^{2-}$ ion in $[\text{PCl}_4]_2[\text{Ti}_2\text{Cl}_{10}]$. Thermal ellipsoids are scaled to include 50% probability.

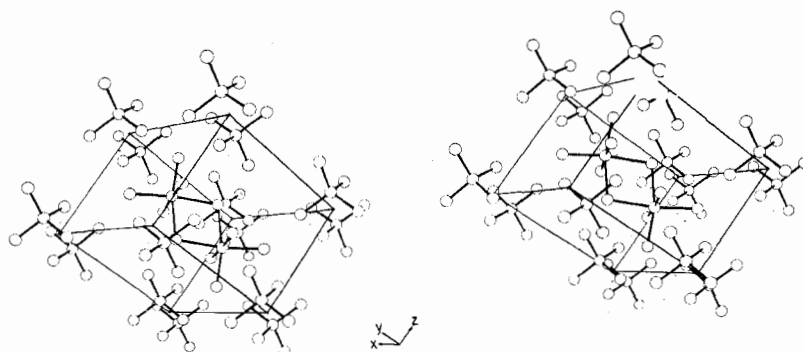


Figure 3.—A stereoview of the arrangement of the unit cell contents for $[\text{PCl}_4]_2[\text{Ti}_2\text{Cl}_{10}]$.

TABLE V
ROOT-MEAN-SQUARE AMPLITUDES OF VIBRATION (Å)
ALONG THE PRINCIPAL AXES, R_i^a

Atom	R_1	R_2	R_3
Ti	0.130 (2)	0.154 (2)	0.183 (2)
Cl(1)	0.151 (3)	0.182 (3)	0.204 (3)
Cl(2)	0.158 (3)	0.202 (3)	0.216 (3)
Cl(3)	0.147 (3)	0.206 (3)	0.221 (3)
Cl(4)	0.147 (3)	0.198 (3)	0.265 (3)
Cl(5)	0.130 (3)	0.157 (2)	0.197 (2)
P	0.143 (3)	0.160 (3)	0.193 (3)
Cl(6)	0.153 (3)	0.194 (3)	0.255 (3)
Cl(7)	0.142 (3)	0.224 (3)	0.253 (3)
Cl(8)	0.178 (3)	0.212 (3)	0.232 (3)
Cl(9)	0.176 (3)	0.193 (3)	0.241 (3)

^a See Figures 1 and 2.

where k and l were both odd. This result was taken to indicate a possible high population of atoms on the mirror planes at $(0, \frac{1}{4}, 0)$ and $(0, \frac{3}{4}, 0)$. As expected, the statistical tests¹¹ reflected this hypersymmetry. Since a sufficiently random distribution of atoms was not present in the unit cell, no definite conclusion about the choice of space group was drawn from the statistical results.

A sharpened, origin-removed Patterson function was calculated using $(E_{hkl}^2 - 1)$ values as coefficients. Assuming the centric group $Pnma$, several attempts were made to interpret the vector map. The map was

characterized by large overlap of vectors and because of this poor resolution and the equiatomic nature of the problem did not yield a sufficient number of correct phases to solve the structure. A symbolic addition¹⁷ solution was attempted and readily provided the correct structure. All 24 atoms in the asymmetric unit were located from an E map. Sixteen of the atoms lie on the mirror at $y = \frac{1}{4}$ and 8 are in general positions. An initial R_1 value calculated from the positions provided by the E map was 0.32. There are two independent PCl_4^+ ions with crystallographic mirror symmetry and two independent $\text{Ti}_2\text{Cl}_{10}^{2-}$ ions, each with crystallographic mirror symmetry. The $\text{Ti}_2\text{Cl}_{10}^{2-}$ ion has the geometry of a face-shared bioctahedron. Refinement in $Pnma$ of the positional and isotropic thermal parameters reduced R_1 to 0.164. At this stage it was evident that some low-angle, high-intensity reflections were severely affected by secondary extinction. Sixteen reflections were removed from the data set for this reason. Several cycles of refinement of the positional and anisotropic thermal parameters gave as final discrepancy factors $R_1 = 0.076$ (observed data) and $R_2 = 0.081$ (observed and unobserved data) for the 1950 reflections of the data set. The estimated standard deviation of an observation of unit weight is 1.84. The function $w(|F_o| - |F_c|)^2$ showed no significant variation with $|F_o|$ or $(\sin \theta)/\lambda$.

TABLE VI
 POSITIONAL AND THERMAL PARAMETERS FOR $[PCl_4][Ti_2Cl_9]$

Atom	<i>x</i>	<i>y</i>	<i>z</i>	<i>B</i> ₁₁ ^a	<i>B</i> ₂₂	<i>B</i> ₃₃	<i>B</i> ₁₂	<i>B</i> ₁₃	<i>B</i> ₂₃
Ti(1)	0.2813 (2) ^b	1/4	0.2383 (3)	0.0013 (1)	0.0054 (4)	0.0026 (3)	0	0.0001 (1)	0
Cl(1)	0.3451 (2)	1/4	0.1327 (5)	0.0009 (1)	0.0103 (8)	0.0059 (5)	0	0.0004 (2)	0
Cl(2)	0.1997 (2)	1/4	0.3006 (4)	0.0012 (1)	0.0091 (7)	0.0045 (5)	0	0.0004 (2)	0
Cl(3)	0.2984 (2)	0.0917 (5)	0.3584 (3)	0.0017 (1)	0.0086 (5)	0.0058 (3)	-0.0002 (2)	-0.0001 (1)	0.0027 (4)
Cl(4)	0.2456 (1)	0.0995 (4)	0.0966 (3)	0.0013 (1)	0.0061 (4)	0.0044 (3)	0.0001 (1)	-0.0001 (1)	-0.0017 (3)
Ti(2)	0.1795 (2)	1/4	0.0867 (3)	0.0012 (1)	0.0082 (5)	0.0047 (3)	0	-0.0004 (1)	0
Cl(5)	0.1299 (2)	0.0921 (5)	0.1098 (4)	0.0015 (1)	0.0086 (6)	0.0104 (5)	-0.0006 (2)	-0.0004 (2)	0.0007 (5)
Cl(6)	0.1833 (3)	1/4	-0.1031 (5)	0.0015 (1)	0.0152 (9)	0.0048 (5)	0	-0.0008 (2)	0
Ti(3)	0.0919 (2)	1/4	0.5852 (4)	0.0013 (1)	0.0107 (6)	0.0041 (3)	0	0.0003 (1)	0
Cl(7)	0.0882 (3)	1/4	0.3951 (5)	0.0015 (1)	0.0381 (21)	0.0044 (6)	0	0.0008 (2)	0
Cl(8)	0.0702 (2)	1/4	0.7994 (4)	0.0014 (1)	0.0096 (7)	0.0034 (4)	0	-0.0007 (2)	0
Cl(9)	0.1401 (2)	0.0914 (6)	0.6120 (5)	0.0015 (1)	0.0130 (7)	0.0133 (6)	0.0011 (2)	-0.0001 (2)	-0.0012 (6)
Cl(10)	0.2571 (2)	0.1012 (5)	0.5939 (4)	0.0015 (1)	0.0131 (6)	0.0074 (4)	-0.0017 (2)	0.0005 (1)	-0.0052 (5)
Ti(4)	-0.0104 (2)	1/4	0.7309 (4)	0.0010 (1)	0.0124 (6)	0.0039 (3)	0	0.0003 (1)	0
Cl(11)	-0.0290 (2)	0.0928 (5)	0.8499 (4)	0.0021 (1)	0.0134 (6)	0.0077 (4)	-0.0015 (2)	0.0012 (2)	0.0020 (5)
Cl(12)	-0.0746 (2)	1/4	0.6229 (6)	0.0011 (1)	0.0363 (9)	0.0060 (6)	0	-0.0004 (2)	0
P(1)	0.3046 (2)	1/4	0.7312 (5)	0.0013 (1)	0.0081 (7)	0.0029 (4)	0	0.0001 (2)	0
Cl(13)	0.3083 (2)	0.1019 (5)	0.8266 (4)	0.0026 (1)	0.0084 (5)	0.0070 (4)	-0.0001 (2)	0.0003 (2)	0.0027 (4)
Cl(14)	0.3549 (2)	1/4	0.6207 (5)	0.0013 (1)	0.0120 (9)	0.0056 (5)	0	0.0006 (2)	0
Cl(15)	0.2478 (3)	1/4	0.6474 (7)	0.0018 (1)	0.0159 (11)	0.0098 (7)	0	-0.0003 (2)	0
P(2)	0.4579 (3)	1/4	0.3111 (5)	0.0013 (1)	0.0121 (9)	0.0037 (5)	0	0.0004 (2)	0
Cl(16)	0.4235 (2)	0.1000 (6)	0.3566 (4)	0.0016 (1)	0.0138 (7)	0.0091 (4)	-0.0008 (2)	-0.0002 (2)	0.0020 (5)
Cl(17)	0.5177 (2)	1/4	0.3845 (5)	0.0015 (1)	0.0122 (8)	0.0061 (6)	0	-0.0008 (2)	0
Cl(18)	0.4661 (3)	1/4	0.1453 (5)	0.0020 (1)	0.0234 (1)	0.0038 (5)	0	0.0008 (2)	0

^a The form of the anisotropic ellipsoid is $\exp[-(B_{11}h^2 + B_{22}k^2 + B_{33}l^2 + 2B_{12}hk + 2B_{13}hl + 2B_{23}kl)]$. ^b Due to uncertainty in the exact model for the structure of $[PCl_4][Ti_2Cl_9]$, the estimated standard deviations quoted here and in Tables VII and VIII may be underestimated.

 TABLE VII
 BOND DISTANCES (Å) AND ANGLES (DEG) FOR $[PCl_4][Ti_2Cl_9]$ ^a

Bond Distances		Terminal-Ti-Terminal Angles	
Ti(1)-Cl(1)	2.221 (7)	Cl(1)-Ti(1)-Cl(3)	98.8 (2)
Ti(1)-Cl(2)	2.480 (8)	Cl(3)-Ti(1)-Cl(3) ^b	97.2 (3)
Ti(1)-Cl(3)	2.221 (5)	Cl(5)-Ti(2)-Cl(5)'	97.0 (3)
Ti(1)-Cl(4)	2.500 (5)	Cl(5)-Ti(2)-Cl(6)	98.8 (2)
Ti(2)-Cl(2)	2.532 (7)	Cl(7)-Ti(3)-Cl(9)	99.9 (2)
Ti(2)-Cl(4)	2.494 (6)	Cl(9)-Ti(3)-Cl(9)'	98.5 (4)
Ti(2)-Cl(5)	2.218 (6)	Cl(11)-Ti(4)-Cl(11)'	96.6 (3)
Ti(2)-Cl(6)	2.188 (7)	Cl(11)-Ti(4)-Cl(12)	98.0 (2)
Ti(3)-Cl(7)	2.192 (8)		Av 98.1 (3)
Ti(3)-Cl(8)	2.546 (6)	Terminal-Ti-Bridge Angles	
Ti(3)-Cl(9)	2.203 (6)	Cl(1)-Ti(1)-Cl(4)	89.5 (2)
Ti(3)-Cl(10)	2.486 (6)	Cl(3)-Ti(1)-Cl(2)	92.0 (2)
Ti(4)-Cl(8)	2.477 (9)	Cl(3)-Ti(1)-Cl(4)	91.4 (2)
Ti(4)-Cl(10)	2.459 (6)	Cl(5)-Ti(2)-Cl(2)	92.0 (2)
Ti(4)-Cl(11)	2.215 (6)	Cl(5)-Ti(2)-Cl(4)	91.2 (2)
Ti(4)-Cl(12)	2.245 (9)	Cl(6)-Ti(2)-Cl(4)	90.4 (2)
P(1)-Cl(13)	1.909 (5)	Cl(7)-Ti(3)-Cl(10)	90.1 (2)
P(1)-Cl(14)	1.940 (9)	Cl(9)-Ti(3)-Cl(8)	91.3 (2)
P(1)-Cl(15)	1.916 (10)	Cl(9)-Ti(3)-Cl(10)	90.7 (2)
P(2)-Cl(16)	1.942 (7)	Cl(11)-Ti(4)-Cl(8)	92.0 (2)
P(2)-Cl(17)	1.935 (9)	Cl(11)-Ti(4)-Cl(10)	91.5 (2)
P(2)-Cl(18)	1.924 (8)	Cl(12)-Ti(4)-Cl(10)	90.1 (2)
			Av 91.0 (2)
Chlorine-P-Chlorine Angles		Bridge-Ti-Bridge Angles	
Cl(13)-P(1)-Cl(14)	109.5 (3)	Cl(2)-Ti(1)-Cl(4)	77.9 (2)
Cl(13)-P(1)-Cl(15)	109.8 (3)	Cl(4)-Ti(1)-Cl(4)'	78.6 (2)
Cl(13)-P(1)-Cl(13)'	109.3 (4)	Cl(2)-Ti(2)-Cl(4)	77.1 (2)
Cl(14)-P(1)-Cl(15)	108.8 (4)	Cl(4)-Ti(2)-Cl(4)'	78.8 (2)
Cl(16)-P(2)-Cl(17)	110.3 (3)	Cl(8)-Ti(3)-Cl(10)	76.6 (2)
Cl(16)-P(2)-Cl(18)	109.4 (3)	Cl(10)-Ti(3)-Cl(10)'	78.1 (3)
Cl(16)-P(2)-Cl(16)'	108.7 (4)	Cl(8)-Ti(4)-Cl(10)	78.4 (2)
Cl(17)-P(2)-Cl(18)	108.8 (5)	Cl(10)-Ti(4)-Cl(10)'	79.1 (3)
			Av 78.1 (3)
Ti-Bridge-Ti Angles			
Ti(1)-Cl(2)-Ti(2)		86.6 (2)	
Ti(1)-Cl(4)-Ti(2)		87.0 (2)	
Ti(3)-Cl(8)-Ti(4)		85.8 (2)	
Ti(3)-Cl(10)-Ti(4)		87.5 (2)	
		Av 86.7 (2)	

^a Errors in the lattice parameters are included in the estimated standard deviations. ^b Primed atoms are symmetry-related to the atoms of the same designation by reflection through the mirror at (0, 1/4, 0).

 TABLE VIII
 SELECTED NONBONDED DISTANCES (Å) FOR $[PCl_4][Ti_2Cl_9]$ ^a

Near-Neighbor Distances within an Ion		Near-Neighbor Distances between Ions	
Ti(1)-Ti(2)	3.439 (6)	Cl(1)-Cl(18)	3.529 (10)
Ti(3)-Ti(4)	3.420 (7)	Cl(2)-Cl(7)	3.427 (10)
Cl(1)-Cl(3)	3.372 (6)	Cl(3)-Cl(16)	3.645 (7)
Cl(1)-Cl(4)	3.329 (7)	Cl(4)-Cl(13)	3.607 (6)
Cl(2)-Cl(3)	3.387 (7)	Cl(5)-Cl(7)	3.876 (8)
Cl(2)-Cl(4)	3.131 (6)	Cl(5)-Cl(17)	3.667 (8)
Cl(2)-Cl(5)	3.424 (7)	Cl(6)-Cl(8)	3.481 (10)
Cl(3)-Cl(3)'	3.331 (9)	Cl(6)-Cl(9)	3.889 (8)
Cl(3)-Cl(4)	3.385 (6)	Cl(6)-Cl(15)	3.432 (10)
Cl(4)-Cl(4)'	3.167 (8)	Cl(7)-Cl(18)	3.585 (12)
Cl(4)-Cl(5)	3.373 (7)	Cl(9)-Cl(15)	3.575 (9)
Cl(4)-Cl(6)	3.330 (7)	Cl(10)-Cl(18)	3.612 (8)
Cl(5)-Cl(5)'	3.322 (10)	Cl(11)-Cl(16)	3.683 (8)
Cl(5)-Cl(6)	3.345 (8)	Cl(11)-Cl(17)	3.643 (6)
Cl(7)-Cl(9)	3.364 (8)	Cl(12)-Cl(18)	3.309 (10)
Cl(7)-Cl(10)	3.317 (8)		
Cl(8)-Cl(9)	3.405 (7)	Near-Neighbor Distances within an Ion	
Cl(8)-Cl(10)	3.119 (6)	Cl(13)-Cl(13)'	3.115 (10)
Cl(8)-Cl(11)	3.380 (8)	Cl(13)-Cl(14)	3.144 (7)
Cl(9)-Cl(9)'	3.338 (12)	Cl(13)-Cl(15)	3.130 (8)
Cl(9)-Cl(10)	3.341 (8)	Cl(14)-Cl(15)	3.135 (11)
Cl(10)-Cl(10)'	3.132 (10)	Cl(16)-Cl(16)'	3.157 (12)
Cl(10)-Cl(11)	3.352 (6)	Cl(16)-Cl(17)	3.182 (8)
Cl(10)-Cl(12)	3.333 (8)	Cl(16)-Cl(18)	3.155 (7)
Cl(11)-Cl(11)'	3.308 (11)	Cl(17)-Cl(18)	3.137 (9)
Cl(11)-Cl(12)	3.367 (8)		

^a See Figure 7.

The results of the refinement in *Pnma* contain a somewhat anomalous feature. Some of the atoms restricted to the mirror in *Pnma* showed excessive anisotropic motion perpendicular to the mirror plane. In an attempt to remove this anomaly three further models were considered: (1) a disordered model in *Pnma* in

TABLE IX
OBSERVED AND CALCULATED STRUCTURE AMPLITUDES FOR $[PCl_4][Ti_2Cl_6]$
[OBS = $10F_o$, CAL = $10F_c$, $F(000) = 22,400$]^a

K	L	OBS	CAL	K	L	OBS	CAL	K	L	OBS	CAL	K	L	OBS	CAL	K	L	OBS	CAL	K	L	OBS	CAL	K	L	OBS	CAL	K	L	OBS	CAL	K	L	OBS	CAL																																																																																																																																																																																																																																																																																																																																																																												
0	0	1822	1800	2	0	206	203	3	10	1073	1119	4	6	296	351	5	6	978	730	6	4	111	148*	7	4	716	880	8	4	716	880	9	4	716	880	10	4	716	880	11	4	716	880	12	4	716	880	13	4	716	880	14	4	716	880	15	4	716	880	16	4	716	880	17	4	716	880	18	4	716	880	19	4	716	880	20	4	716	880	21	4	716	880	22	4	716	880	23	4	716	880	24	4	716	880	25	4	716	880	26	4	716	880	27	4	716	880	28	4	716	880	29	4	716	880	30	4	716	880	31	4	716	880	32	4	716	880	33	4	716	880	34	4	716	880	35	4	716	880	36	4	716	880	37	4	716	880	38	4	716	880	39	4	716	880	40	4	716	880	41	4	716	880	42	4	716	880	43	4	716	880	44	4	716	880	45	4	716	880	46	4	716	880	47	4	716	880	48	4	716	880	49	4	716	880	50	4	716	880	51	4	716	880	52	4	716	880	53	4	716	880	54	4	716	880	55	4	716	880	56	4	716	880	57	4	716	880	58	4	716	880	59	4	716	880	60	4	716	880	61	4	716	880	62	4	716	880	63	4	716	880	64	4	716	880	65	4	716	880	66	4	716	880	67	4	716	880	68	4	716	880	69	4	716	880	70	4	716	880	71	4	716	880	72	4	716	880	73	4	716	880	74	4	716	880	75	4	716	880	76	4	716	880	77	4	716	880	78	4	716	880	79	4	716	880	80	4	716	880	81	4	716	880	82	4	716	880	83	4	716	880	84	4	716	880	85	4	716	880	86	4	716	880	87	4	716	880	88	4	716	880	89	4	716	880	90	4	716	880	91	4	716	880	92	4	716	880	93	4	716	880	94	4	716	880	95	4	716	880	96	4	716	880	97	4	716	880	98	4	716	880	99	4	716	880	100	4	716	880

^a Unobserved reflections are indicated with an asterisk.

which all 16 of the atoms restricted to $y = 1/4$ were moved off the mirror, (2) a disordered model in $Pnma$ in which only the titanium and phosphorus atoms were restricted to the mirror at $y = 1/4$, and (3) refinement in the acentric space group $Pn2_1a$. In the refinement of the disordered models, some atoms which had pre-

viously been restricted to $y = 1/4$ moved a substantial distance off the mirror (0.10-0.20 Å) leading to unrealistic bond distances and angles. These atoms also displayed nonpositive definite temperature factors. The acentric model proceeded slowly through isotropic refinement and provided a slightly lower R_1 value than

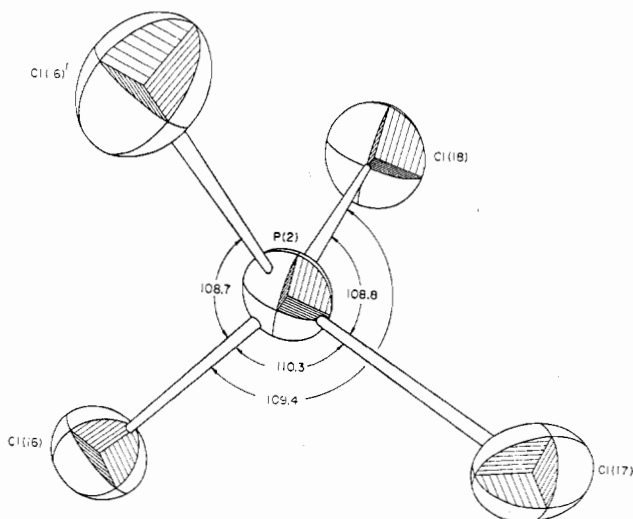


Figure 4.—A perspective view of the coordination geometry of one of the independent PCl_4^+ ions in $[\text{PCl}_4][\text{Ti}_2\text{Cl}_9]$. Thermal ellipsoids are scaled to include 50% probability.

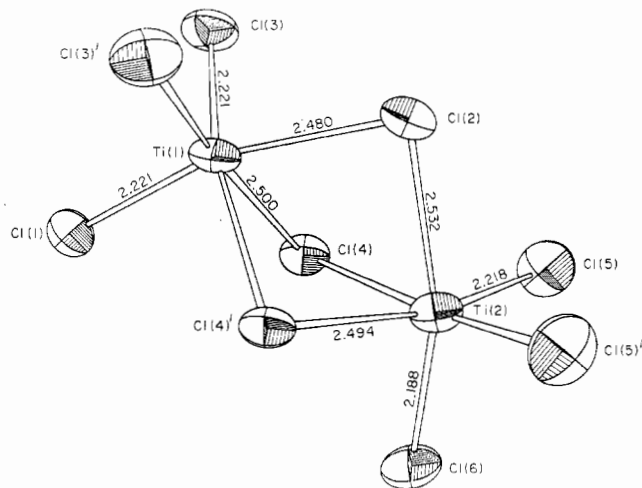


Figure 5.—A perspective view of the $\text{Ti}(1)$ – $\text{Ti}(2)$ bioctahedron in $[\text{PCl}_4][\text{Ti}_2\text{Cl}_9]$. Thermal ellipsoids are scaled to include 50% probability.

the ordered centric model. However, upon anisotropic refinement some of the atoms developed non-positive definite thermal parameters. In view of the experimental difficulties encountered in data collection and the relatively low ratio of observations to variables in the disordered and acentric models, it is felt that we cannot conclusively rule out these models on the basis of the above refinements. However, the calculations based on the ordered centric model provide a fairly accurate fit of the experimental data, and the results of that refinement are reported here. Table VI gives the positional and thermal parameters derived from the final anisotropic refinement in $Pnma$. Tables VII and VIII contain summaries of the bond distances and angles and nonbonded contact distances. The observed and calculated structure amplitudes are compared in Table IX. The magnitudes of the root-mean-

TABLE X
ROOT-MEAN-SQUARE AMPLITUDES OF VIBRATION (\AA)
ALONG THE PRINCIPAL AXES, R_i^a

Atom	R_1	R_2	R_3
Ti(1)	0.132 (7)	0.173 (7)	0.238 (7)
Cl(1)	0.180 (10)	0.214 (9)	0.241 (9)
Cl(2)	0.169 (9)	0.226 (9)	0.232 (9)
Cl(3)	0.163 (7)	0.245 (6)	0.275 (6)
Cl(4)	0.146 (8)	0.205 (6)	0.240 (6)
Ti(2)	0.170 (7)	0.215 (6)	0.230 (7)
Cl(5)	0.209 (7)	0.250 (6)	0.278 (7)
Cl(6)	0.167 (10)	0.264 (10)	0.292 (9)
Ti(3)	0.164 (6)	0.235 (7)	0.245 (7)
Cl(7)	0.159 (12)	0.265 (12)	0.463 (12)
Cl(8)	0.139 (10)	0.232 (9)	0.249 (9)
Cl(9)	0.226 (8)	0.286 (7)	0.307 (7)
Cl(10)	0.160 (8)	0.230 (7)	0.333 (7)
Ti(4)	0.159 (7)	0.215 (7)	0.264 (6)
Cl(11)	0.180 (8)	0.276 (7)	0.330 (7)
Cl(12)	0.191 (11)	0.226 (11)	0.452 (12)
P(1)	0.140 (10)	0.213 (9)	0.240 (9)
Cl(13)	0.173 (7)	0.252 (7)	0.333 (7)
Cl(14)	0.183 (9)	0.248 (9)	0.260 (9)
Cl(15)	0.252 (9)	0.282 (11)	0.298 (10)
P(2)	0.153 (11)	0.236 (10)	0.261 (9)
Cl(16)	0.231 (7)	0.251 (7)	0.302 (7)
Cl(17)	0.186 (10)	0.262 (9)	0.269 (10)
Cl(18)	0.150 (11)	0.299 (10)	0.362 (10)

^a See Figures 4–6.

square displacements for all atoms are given in Table X. Figure 4 is a view of one of the independent PCl_4^+ ions, and Figures 5 and 6 are views of the two independent Ti_2Cl_9^- ions. A perspective view down $[010]$ of the arrangement of the ions in the $y = 1/4$ plane is given in Figure 7. A final difference map showed no peaks higher than $1.5 \text{ e}^-/\text{\AA}^3$ and had an average background of $0.5 \text{ e}^-/\text{\AA}^3$.

Discussion

The geometry of the $\text{Ti}_2\text{Cl}_{10}^{2-}$ ion in $[\text{PCl}_4]_2[\text{Ti}_2\text{Cl}_{10}]$ is similar to that of the edge-bridged dimer found in the structure of $[\text{POCl}_3 \cdot \text{TiCl}_4]_2$ reported by Branden and Lindquist.¹⁹ The four-membered bridge system is nearly identical in the two structures (Cl–Ti–Cl angles of 78.5 (3) and 78.78 (8) $^\circ$ and Ti–Cl(bridge)–Ti angles of 101.5 (4) and 101.21 (9) $^\circ$, respectively, for $\text{Ti}_2\text{Cl}_{10}^{2-}$ and the POCl_3 complex). The Ti–Cl(bridge) distances are considerably less asymmetric in the ion than in the molecular dimer (2.481 (2) and 2.506 (2) \AA vs. 2.44 (1) and 2.54 (1) \AA). The Cl–Cl bridge distances in the $\text{Ti}_2\text{Cl}_{10}^{2-}$, Ti_2Cl_9^- , and $[\text{POCl}_3 \cdot \text{TiCl}_4]_2$ species average 3.16 \AA . This is nearly identical with the average Cl–Cl bridge distance (3.17 \AA) previously reported^{20a} for other chlorine-bridged compounds and further supports our suggestion that Cl–Cl bridge interactions are primarily responsible for determining bridge geometries in many chlorine-bridged systems. We also note that the average Cl–Cl bridge distance is approximately 0.20 \AA less than the nonbridging Cl–Cl distances and 0.44 \AA less than the normal van der Waals Cl–Cl ap-

(19) C. I. Branden and I. Lindquist, *Acta Chem. Scand.*, **14**, 726 (1960).

(20) (a) F. K. Ross and G. D. Stucky, *J. Amer. Chem. Soc.*, **92**, 4538 (1970); (b) K. Mucker, G. S. Smith, and Q. Johnson, *Acta Crystallogr., Sect. B*, **24**, 874 (1968).

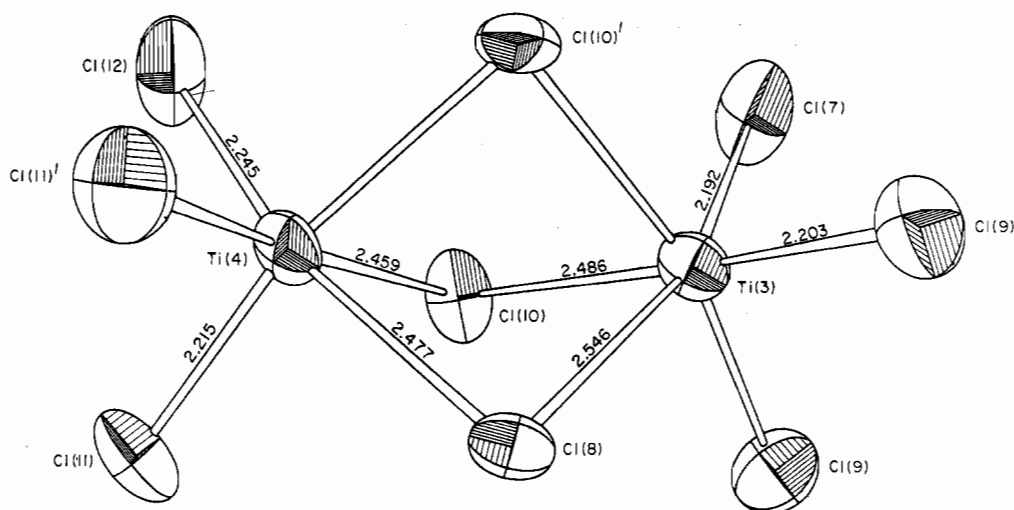


Figure 6.—A perspective view of the Ti(3)–Ti(4) bioctahedron in $[\text{PCl}_4][\text{Ti}_2\text{Cl}_9]$. Thermal ellipsoids are scaled to include 50% probability.

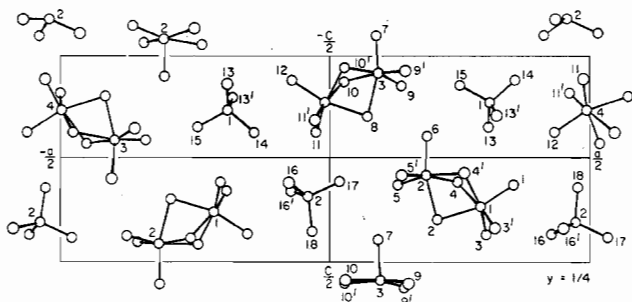


Figure 7.—A perspective view down $[010]$ of the arrangement of the ions in the $y = 1/4$ plane for $[\text{PCl}_4][\text{Ti}_2\text{Cl}_9]$.

proach (3.60 Å). The bridging chlorine atoms are situated between two strong electropositive centers and can be expected to be more like Cl^0 and less like Cl^- than are the nonbridging chlorine atoms. Our earlier tentative suggestion^{20a} that the asymmetry in the (M–Cl) bridged distances is caused by intra-ring metal–metal repulsions does not appear to be correct since, if the nonbridging ligands are ignored, symmetry arguments require that all metal–chlorine bridge distances be the same. This means that the bridge asymmetry must be due to asymmetry introduced into the molecule by bonding and nonbonding interactions involving the nonbridging ligands and/or lattice effects. The Ti atoms do not lie at the centers of the octahedra and this accounts for the variance of the Cl(terminal)–Ti–Cl(terminal) angles from 90° .

The molecular geometry of $\text{Ti}_2\text{Cl}_{10}^{2-}$ is very similar to that exhibited by $\text{Re}_2\text{Cl}_{10}$.^{20b} The terminal equatorial Ti–Cl distances 2.247 (2) and 2.269 (2) Å are to be compared to the average of eight terminal Re–Cl distances of 2.244 (12) Å. There is no significant difference in the axial and equatorial Re–Cl bond lengths in $\text{Re}_2\text{Cl}_{10}$, while the axial lengths in $\text{Ti}_2\text{Cl}_{10}^{2-}$ are ~ 0.05 Å longer than the equatorial lengths due to steric and Coulombic interactions with the PCl_4^+ ions (see Figure 3). Somewhat surprising perhaps is the fact that the repulsion between the Re^{5+} centers appears to be somewhat less than between the Ti^{4+} centers as evidenced by the shorter metal–metal distance

(3.739 vs. 3.855 Å), the larger Cl(bridge)–metal–Cl(bridge) angles (81° as compared to 79°), and the smaller shift of the metal atom from the center of the octahedra in the Re compound. This is probably due to the higher degree of covalency in the rhenium compound than in the titanium compound and a subsequent reduction in the metal–metal repulsions.

Reich and Wieker²¹ on the basis of infrared and Raman studies have concluded that the adduct $\text{PCl}_5 \cdot \text{SnCl}_4$ should be formulated as $[\text{PCl}_4]_2[\text{Sn}_2\text{Cl}_{10}]$ with a structure exactly analogous to that found here for $[\text{PCl}_4]_2[\text{Ti}_2\text{Cl}_{10}]$.

The occurrence of Ti_2Cl_9^- in $[\text{PCl}_4][\text{Ti}_2\text{Cl}_9]$ is the first X-ray confirmation of a first-row transition metal in the +4 formal oxidation state to assume the geometry of the face-shared bioctahedron. However, Creighton and Green²² have recently reported the existence of the Ti_2Cl_9^- ion in $[(\text{C}_2\text{H}_5)_4\text{N}][\text{Ti}_2\text{Cl}_9]$ on the basis of infrared data. The two crystallographically independent Ti_2Cl_9^- ions have very similar sets of bond distances and angles. The distortions from octahedral geometry observed in Ti_2Cl_9^- are typical of bridged metal–metal systems with no metal–metal bonding.²³ The average Cl–Cl distance in the shared face is 3.137 (9) Å, while that for the terminal chlorines is 3.343 (8) Å. This unusually close Cl–Cl contact can be compared to that found in the $\text{Ti}_2\text{Cl}_{10}^{2-}$ edge-shared ion of 3.165 (3) Å. The average Cl(bridge)–Ti–Cl(bridge) angle has closed to $78.1 (3)^\circ$, while the average Cl(terminal)–Ti–Cl(terminal) angle has opened to $98.1 (3)^\circ$. The sharing of faces in this ion has considerably shortened the Ti–Ti distance (3.439 (6) and 3.420 (7) Å) compared to the edge-bridged ion (3.855 (3) Å).

Table XI contains a summary of the thermally corrected terminal titanium–chlorine bond distances in $\text{Ti}_2\text{Cl}_{10}^{2-}$ and Ti_2Cl_9^- . The riding model of Busing and Levy²⁴ has been used in the thermal analysis since it was felt that it provides a good representation for the

(21) P. Reich and W. Wieker, *Z. Naturforsch. B*, **23**, 739 (1968).

(22) J. A. Creighton and J. H. S. Green, *J. Chem. Soc. A*, 808 (1968).

(23) F. A. Cotton, *Rev. Pure Appl. Chem.*, **17**, 25 (1967).

(24) W. R. Busing and H. A. Levy, *Acta Crystallogr.*, **17**, 142 (1964).

covalent structure of the titanium–chlorine bond. As has been previously mentioned, the axial Ti–Cl bond lengths in the $Ti_2Cl_{10}^{2-}$ edge-bridged ion are significantly longer than the equatorial bonds and remain so after thermal correction. The average lengthening of the Ti–Cl bonds is approximately 0.01 Å due to thermal motion.

TABLE XI
TERMINAL TITANIUM–CHLORINE BOND DISTANCES IN
 $Ti_2Cl_{10}^{2-}$ AND $Ti_2Cl_9^-$

	Uncor- rected	Riding model		Uncor- rected	Riding model
[PCl_4] ₂ [Ti_2Cl_{10}], Site Symmetry 1					
Ti–Cl(1)	2.300 (3)	2.305 (3)	Ti–Cl(3)	2.247 (2)	2.256 (2)
Ti–Cl(2)	2.291 (3)	2.299 (3)	Ti–Cl(4)	2.269 (2)	2.281 (2)
[PCl_4][Ti_2Cl_9], Site Symmetry <i>m</i>					
Ti(1)–Cl(1)	2.221 (7)	2.230 (7)	Ti(3)–Cl(7)	2.192 (7)	2.229 (8)
Ti(1)–Cl(3)	2.221 (5)	2.233 (5)	Ti(3)–Cl(9)	2.203 (6)	2.224 (6)
Ti(2)–Cl(5)	2.218 (6)	2.231 (6)	Ti(4)–Cl(11)	2.215 (6)	2.234 (6)
Ti(2)–Cl(6)	2.188 (7)	2.200 (7)	Ti(4)–Cl(12)	2.245 (9)	2.280 (9)

There are no symmetry requirements on the PCl_4^+ ion in [PCl_4]₂[Ti_2Cl_{10}]. The molecular symmetry of PCl_4^+ is, however, very nearly tetrahedral. The two independent PCl_4^+ ions in the structure of [PCl_4]-[Ti_2Cl_9] exhibit the same nearly tetrahedral symmetry as found in [PCl_4][$FeCl_4$]²⁵ and [PCl_4]₂[Ti_2Cl_{10}].

As a result of the structural studies of [PCl_4][$FeCl_4$]²⁵ [PCl_4]₂[Ti_2Cl_{10}], and [PCl_4][Ti_2Cl_9], we have observed the tetrachlorophosphonium ion in a variety of crystal structures. The crystallographic site symmetry in no individual case is required to be higher than mirror symmetry. Of the 18 independent angles found in the three structures, the maximum deviation from the ideal tetrahedral angle of 109.5° is 1.2° found in [PCl_4]-[$FeCl_4$]. The PCl_4^+ ion in this structure shows the largest corrections for thermal motion. Since bond angles cannot be corrected for thermal motion using the approximations applicable to bond lengths,²⁴ this deviation may in part be due to a lack of consideration of the thermal effects. The 12 independent P–Cl bond distances observed in the three structures have been corrected for shortening due to thermal motion using the riding model of Busing and Levy²⁴ and are compared in Table XII. There are two major features to be considered: (1) the order of magnitude of the correction varies both among structures and within a structure, and (2) the bond distances have converged upon correction for thermal motion. The average of these 12 corrected distances is 1.944 (6) Å. This value represents the best approximation for the phosphorus–chlorine bond distance in the PCl_4^+ ion.

As has been previously mentioned in the Introduction, the reaction of PCl_5 and $TiCl_4$ in $POCl_3$ and the reaction of PCl_3 , $SOCl_2$, and $TiCl_4$ in $SOCl_2$ were both reported³ to give a compound of empirical formula $PTiCl_9$. We have found, however, that the second reaction yields [PCl_4][Ti_2Cl_9] rather than [PCl_4]₂[Ti_2Cl_{10}]. Before proceeding to a discussion of the factors that may be involved with this result, one further result

(25) T. J. Kistenmacher and G. D. Stucky, *Inorg. Chem.*, **7**, 2150 (1968).

TABLE XII
PHOSPHORUS–CHLORINE BOND DISTANCES IN THE PCl_4^+ ION

	Uncorrected	Riding model	Site sym- metry
[PCl_4][$FeCl_4$] ^a			
P–Cl(4)	1.912 (1)	1.951 (1)	2
P–Cl(5)	1.902 (1)	1.942 (1)	
[PCl_4] ₂ [Ti_2Cl_{10}]			
P–Cl(6)	1.924 (3)	1.935 (3)	1
P–Cl(7)	1.936 (3)	1.949 (3)	
P–Cl(8)	1.936 (3)	1.948 (3)	
P–Cl(9)	1.924 (3)	1.936 (3)	
[PCl_4][Ti_2Cl_9]			
P(1)–Cl(13)	1.909 (5)	1.932 (6)	<i>m</i>
P(1)–Cl(14)	1.940 (9)	1.950 (9)	
P(1)–Cl(15)	1.916 (10)	1.939 (10)	
P(2)–Cl(16)	1.942 (7)	1.958 (7)	
P(2)–Cl(17)	1.935 (9)	1.944 (9)	
P(2)–Cl(18)	1.924 (8)	1.949 (8)	
[PCl_4][PCl_6] ^b			
P(I)–Cl(III)	~1.97		$\bar{4}$
[PCl_4][$ClICl$] ^c			
P–Cl	1.98		$\bar{4}$

^a Reference 25. ^b D. Clark, H. M. Powell, and A. F. Wells, *J. Chem. Soc.*, 642 (1942). ^c W. F. Zelezny and N. C. Baenziger, *J. Amer. Chem. Soc.*, **74**, 6151 (1952).

will be described. In the Experimental Section a third reaction besides the two used to provide crystals for the X-ray analyses is given. In this reaction $PCl_5(s)$ was allowed to react with $TiCl_4$ in $SOCl_2$ and yielded [PCl_4]-[Ti_2Cl_9]. This result coupled with the other synthetic data leads to the conclusions that the reaction of PCl_5 and $TiCl_4$ in $POCl_3$ yields the 1:1 adduct, that the reaction of PCl_5 and $TiCl_4$ in $SOCl_2$ yields the $PCl_5 \cdot 2TiCl_4$ adduct, and that the product is independent of the method of introduction of the PCl_5 (as solid PCl_5 or by the reaction of PCl_3 with $SOCl_2$). The solvent is apparently the dominating force in the selection of the stoichiometry and geometry of the anion formed. There are two solvent characteristics of major importance: (1) dielectric constant and (2) coordinating ability. The dielectric constants for $SOCl_2$ and $POCl_3$ are 9.25 and 13.3. The formation of the dinegative $Ti_2Cl_{10}^{2-}$ would certainly be more favorable in the higher dielectric solvent ($POCl_3$) as is found to be the case. However, the strongest force determining which anion is formed is probably the coordinating ability of the solvent. Sheldon and Tyree²⁶ have shown on the basis of freezing point diagrams and infrared data that $POCl_3$ is a much stronger base toward $TiCl_4$ than $SOCl_2$. The formation of solvated species has been shown to be of importance in nonaqueous solvent systems.²⁷ Although we have no specific information on the number or kind of solvated species formed in the reaction systems studied here, the formation of solvated species such as the dimeric form of $POCl_3 \cdot TiCl_4$ would certainly sterically hinder the formation of the face-shared bioctahedron and favor the edge-bridged dimer.

(26) J. C. Sheldon and S. Y. Tyree, Jr., *J. Amer. Chem. Soc.*, **81**, 2290 (1959).

(27) R. S. Drago and K. F. Purcell, *Prog. Inorg. Chem.*, **6**, 271 (1964).